

LHC Signatures of New Gauge Bosons in the Minimal Higgsless Model

Hong-Jian He¹, Yu-Ping Kuang¹, Yong-Hui Qi¹, Bin Zhang¹

¹Center for High Energy Physics, Tsinghua University, Beijing 100084, China

Alexander Belyaev², R. Sekhar Chivukula², Neil D. Christensen², Alexander Pukhov³, Elizabeth H. Simmons²

²Department of Physics and Astronomy, Michigan State University, East Lansing, MI 48824, USA

³Skobeltsyn Institute of Nuclear Physics, Moscow State University, Moscow 119992, Russia

We study the LHC signatures of new gauge bosons in the gauge-invariant minimal Higgsless model. It predicts an extra pair of W_1 and Z_1 bosons which can be as light as ~ 400 GeV and play a key role in the delay of unitarity violation. We analyze the W_1 signals in $pp \rightarrow W_0 Z_0 Z_0 \rightarrow jj4\ell$ and $pp \rightarrow W_0 Z_0 jj \rightarrow \nu 3\ell jj$ processes at the LHC, including the complete electroweak and QCD backgrounds. We reveal the complementarity between these two channels for discovering the W_1 boson, and demonstrate the LHC discovery potential over the full range of allowed W_1 mass.

PACS: 12.60.Cn, 11.10.Kk, 12.15.Ji, 13.85.Qk

arXiv: 0708.2588 [hep-ph]

1. Introduction

Unraveling the mechanism of electroweak symmetry breaking (EWSB) is the most pressing task facing particle physics today, and is a major driving force behind the CERN Large Hadron Collider (LHC). New spin-1 gauge bosons serve as the key for Higgsless EWSB [1], by delaying unitarity violation of longitudinal weak boson scattering up to a higher ultraviolet scale [2, 3] without invoking a fundamental Higgs scalar [4]. Dimensional deconstruction [5] was shown to provide the most general *gauge-invariant* formulation [3, 6] of Higgsless theories under arbitrary geometry of the continuum fifth dimension (5d) or its 4d discretization with only a few lattice sites [7, 8]. The Minimal Higgsless Model (MHLM) consists of just 3 lattice sites (“The Three Site Model”) [8], and includes extra nearly degenerate (W_1 , Z_1) bosons which are allowed by precision data to be as light as ~ 400 GeV [8]. The model contains all the essential ingredients of Higgsless theories, and is the simplest realistic Higgsless model with distinct collider signatures. In this paper we study the LHC signatures of the new W_1 boson via processes $pp \rightarrow W_0 Z_0 Z_0 \rightarrow jj4\ell$ and $pp \rightarrow W_0 Z_0 jj \rightarrow \nu 3\ell jj$, where (W_0 , Z_0) are the light weak gauge bosons analogous to those in the standard model (SM). The MHLM is exactly gauge-invariant with spontaneous gauge symmetry breaking, hence it allows our analysis to predict consistent high-energy behavior for any relevant scattering amplitude, contrary to the previous gauge-noninvariant calculation in a naive 5d Higgsless sum rule approach [9].

2. Model Setup and Delayed Unitarity Violation

The MHLM [8] is defined as a chain moose with 3 lattice sites, under the gauge groups $SU(2)_0 \otimes SU(2)_1 \otimes U(1)_2$ [10]. Its gauge and Goldstone sectors have 5 parameters in total — 3 gauge couplings (g_0 , g_1 , g_2) and 2 Goldstone decay constants (f_1 , f_2), satisfying two conditions due to its symmetry breaking structure,

$$\frac{1}{g_0^2} + \frac{1}{g_1^2} + \frac{1}{g_2^2} = \frac{1}{e^2}, \quad \frac{1}{f_1^2} + \frac{1}{f_2^2} = \frac{1}{v^2}. \quad (1)$$

For the optimal delay of unitarity violation we will choose equal decay constants $f_1 = f_2 = \sqrt{2}v$ where $v = (\sqrt{2}G_F)^{-1/2}$ as fixed by the Fermi constant. Inputting two gauge boson masses, e.g., the light gauge boson mass $M_{W0} \simeq 80$ GeV and new gauge boson mass M_{W1} , we can determine all three gauge couplings (g_0 , g_1 , g_2).

The MHLM exhibits a delay of unitarity violation in light weak boson scattering $V_{0L}^a V_{0L}^b \rightarrow V_{0L}^c V_{0L}^d$ ($V_0 = W_0, Z_0$). The scattering $W_{0L} Z_{0L} \rightarrow W_{0L} Z_{0L}$ is related to our collider study, so we derive the corresponding unitarity limits, $E^* \simeq 3.1, 2.95, 2.8, 2.55, 2.35, 1.7$ TeV for $M_{W1} = 0.4, 0.5, 0.6, 0.8, 1.0, \infty$ TeV, respectively. (We have also analyzed the unitarity limit in the combined isospin-0 channel and find somewhat tighter limits: $E^* = 2.0, 1.86, 1.74, 1.66, 1.45, 1.2$ TeV, for $M_{W1} = 0.4, 0.5, 0.6, 0.8, 1.0, \infty$ TeV, respectively.) So, for $M_{W1} \lesssim 1$ TeV, each elastic $V_{0L} V_{0L}$ scattering remains unitary over the main energy range of the LHC.

The fermion sector contains SM-like chiral fermions: left-handed doublets ψ_{0L} under $SU(2)_0$ and right-handed weak singlets ψ_{2R} . For each flavor of ψ_{0L} , there is a heavy vector-fermion doublet Ψ_1 under $SU(2)_1$. The mass matrix for $\{\psi, \Psi\}$ is [8]

$$M_F = \begin{pmatrix} m & 0 \\ M & m' \end{pmatrix} \equiv M \begin{pmatrix} \epsilon_L & 0 \\ 1 & \epsilon_R \end{pmatrix}. \quad (2)$$

The light SM fermions acquire small masses proportional to ϵ_R . For the present high energy scattering analysis we only need to consider light SM fermions relevant to the proton structure functions at the LHC, which can be treated as massless to good accuracy. So we will set $\epsilon_R \simeq 0$, implying that ψ_{2R} and Ψ_1 do not mix. The mass-diagonalization of M_F yields a nearly massless SM-like light fermion F_0 and a heavy new fermion F_1 of mass $M_{F_1} = M\sqrt{1+\epsilon_L^2}$. The low energy constraints already put a strong lower bound on the heavy fermion mass, $M_{F_1} > 1.8$ TeV [8]. Hence we focus our analysis on the production and detection of the new gauge boson W_1 (Z_1) which can be as light as ~ 400 GeV. To simplify the analysis we will consistently decouple the heavy fermion by

taking the limit $(M, m) \rightarrow \infty$ while keeping the ratio $\epsilon_L \equiv m/M$ finite. This finite ratio ϵ_L will be fixed via the ideal fermion delocalization [11], leading to vanishing W_1 -fermion couplings and thus zero electroweak precision corrections at tree-level [8, 11]. We stress that the precisely defined fermion gauge couplings as well as gauge-boson self-couplings in the MHLM [8] are the key to ensuring exact gauge-invariance in our collider study below. This feature makes our analysis essentially different from Ref. [9] which relies on a naive 5d Higgsless sum rule approach where both the fermion gauge couplings and the deviations of the W_0/Z_0 self-couplings from the SM cannot be correctly derived.

3. Discovering the W_1 Boson via $pp \rightarrow W_0 Z_0 Z_0$

Since W_1 has vanishing fermionic couplings in the MHLM due to ideal fermion-delocalization [8, 11], it decays to $W_0 Z_0$ only, with the total width,

$$\Gamma_{W_1} = \frac{\alpha M_{W_1}^3}{192 s_Z^2 M_{W_0}^2} \left[1 + \frac{9+7c_Z^2}{c_Z^2} r^2 + O(r^4) \right] \quad (3)$$

where $\alpha = e^2/4\pi$ and $r \equiv M_{W_0}/M_{W_1} \ll 1$. We note that in Eq.(3) the total width at the leading order (r^0) comes from the purely longitudinal decay mode $W_{1L} \rightarrow W_{0L}Z_{0L}$ alone. Typically, we have $\Gamma_{W_1} \simeq (3, 5, 17, 31)$ GeV for $M_{W_1} = (0.4, 0.5, 0.8, 1)$ TeV.

In this and next sections our collider studies will be performed at the parton-level (unless specified otherwise). Now we study the new process $pp \rightarrow W_0 Z_0 Z_0$ at the LHC, where the signal comes from $pp \rightarrow W_0^* \rightarrow W_1^{(*)} Z_0 \rightarrow W_0 Z_0 Z_0$. We propose to analyze the final state detection via leptonic decays of the two Z_0 bosons and hadronic decays of W_0 . This gives rise to a clean signature of 4-leptons plus 2-jets, $jj\ell^+\ell^-\ell^+\ell^-$ ($\ell = e, \mu$, $jj = qq'$). The backgrounds include: (a) the irreducible SM production of $pp \rightarrow W_0 Z_0 Z_0 \rightarrow jj\ell^+\ell^-\ell^+\ell^-$ ($jj = qq'$, without W_1 contribution), (b) the reducible background of the SM production, $pp \rightarrow Z_0 Z_0 Z_0 \rightarrow jj\ell^+\ell^-\ell^+\ell^-$ ($jj = q\bar{q}$), with one $Z_0 \rightarrow jj$ (mis-identified as W_0) since the mass-splitting $M_{Z_0} - M_{W_0}$ is within the uncertainty of reconstructing the W_0 boson, and (c) the SM process $pp \rightarrow jj\ell^+\ell^-\ell^+\ell^-$ other than (a) and (b), which also includes the $jj4\ell$ backgrounds with $jj = qq, gg$.

We first impose the following cuts for particle identifications

$$\begin{aligned} p_{T\ell} > 10 \text{ GeV}, & \quad |\eta_\ell| < 2.5, \\ p_{Tj} > 15 \text{ GeV}, & \quad |\eta_j| < 4.5. \end{aligned} \quad (4)$$

To suppress the backgrounds, we further impose

$$\begin{aligned} M_{jj} &= 80 \pm 15 \text{ GeV}, \quad \Delta R(jj) < 1.5, \\ \sum_{i=1}^2 p_T(Z_i) + \sum_{i=1}^2 p_T(j_i) &= \pm 15 \text{ GeV}. \end{aligned} \quad (5)$$

The M_{jj} cut is the requirement of reconstructing W_0 from the dijets (due to on-shell W_0 decay) according to the experimental resolution ± 15 GeV [12]. The $\Delta R(jj)$ cut is for suppressing the $jj = qq, gg$ backgrounds.

In practical data analyses for reconstructing W_0 , there is no need to require separation between the two jets. Then there can be a background from a single jet or overlapping jet pair (arising from a single parton) with invariant-mass satisfying the M_{jj} requirement (5) which may mimic the two unseparated jets. So we need to impose a further cut to suppress this background. With a detailed simulation study using PYTHIA with the k_T algorithm (taking the default parameter $d_{cut} = \sqrt{s}$) and considering showering effects, we find that the cut requiring p_T balance can suppress the single-jet background to the level of 10^{-2} events which is invisible in FIG. 1.

The relevant SM backgrounds are simulated using the Madgraph package [13] and a few related ones [14].

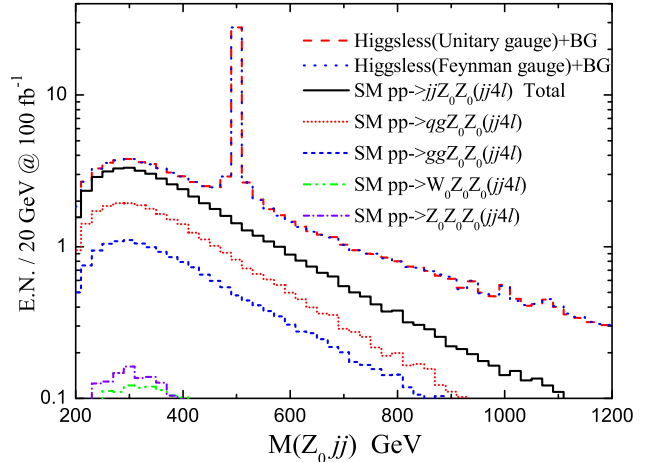


FIG. 1: Signal and background events in the process $pp \rightarrow W_1^{(*)} Z_0 \rightarrow W_0 Z_0 Z_0 \rightarrow jj\ell^+\ell^-\ell^+\ell^-$ for an integrated luminosity of 100 fb^{-1} .

We plot the signal and background events under these cuts for an integrated luminosity of 100 fb^{-1} in Fig. 1, where we depict the signal by a dashed curve, the backgrounds (c) with $jj = gg, q\bar{q}$ by small-dashed and small-dotted curves, respectively. The backgrounds (a) and (b) with $jj = qq, q\bar{q}$ are much smaller, appearing marginally on the left-lower corner of Fig. 1. We summarize the total backgrounds (a)+(b)+(c), depicted by the solid curve in Fig. 1. We define the signal to include all events in the region $M_{Zjj} = M_{W_1} \pm 0.04M_{W_1}$, where the backgrounds are much smaller than the signal. The final state $W_0 Z_0 Z_0$ contains two identical Z_0 bosons and we have summed up the contributions from the two combinations of M_{Zjj} for all the curves in Fig. 1. For the signal curve, the non-resonant region on the right-hand-side of the peak mainly comes from the contributions of the two Zjj -combinations including no W_1 peak; this region also decreases more slowly than the other backgrounds. The gauge-invariance of this calculation is verified by comparing the signal distributions in unitary and 't Hooft-Feynman gauges; as shown in Fig. 1 by red-dashed and

blue-dotted curves, they perfectly coincide. We further derive statistical significance from Poisson probability in the conventional way. The integrated luminosity required for detecting the new W_1 gauge bosons in this channel will be summarized in Fig. 4 as a function of mass M_{W_1} .

4. Discovering the W_1 Boson via $pp \rightarrow W_0 Z_0 jj$

Next, we analyze the discovery of W_1 bosons in the process $pp \rightarrow W_0 Z_0 qq'$, where the signal is given by the W_1 contribution to the $W_0 Z_0 \rightarrow W_0 Z_0$ subprocess. We perform a complete analysis of $pp \rightarrow W_0 Z_0 jj$, and choose the pure leptonic decay modes of $W_0 Z_0$ with 3 leptons plus missing- E_T [15, 16]. We carry out the first full $2 \rightarrow 4$ calculation for the MHLML, including both the electroweak (EW) and QCD backgrounds for $pp \rightarrow W_0 Z_0 jj$. We find the total SM backgrounds to be an order of magnitude larger than those estimated in [9].

We first analyze how to suppress the SM backgrounds. We employ a forward-jet tag to eliminate the annihilation process $qq' \rightarrow W_0 Z_0$ (with possible QCD-jet radiation), as a reducible QCD background [15]. Of greater concern are the reducible QCD backgrounds $pp \rightarrow W_0 Z_0 jj$ with $jj = qg, gg$ serving as forward jets. We find that these two QCD backgrounds are quite significant even under the cuts of [9, 15]. Hence we employ the following improved cuts to more effectively suppress the backgrounds,

$$E_j > 300 \text{ GeV}, \quad p_{Tj} > 30 \text{ GeV}, \quad (6)$$

$$|\eta_j| < 4.5, \quad |\Delta\eta_{jj}| > 4, \quad (7)$$

where E_j and p_{Tj} are transverse energy and momentum of each final-state jet, η_j is the forward jet rapidity, and $|\Delta\eta_{jj}|$ is the difference between the rapidities of the two forward jets. The cut on $|\Delta\eta_{jj}|$ suppresses [17] the QCD backgrounds $pp \rightarrow W_0 Z_0 gg, W_0 Z_0 qg$, especially in the low $M_{W_0 Z_0}$ region. In addition, we employ the following lepton identification cuts,

$$p_{T\ell} > 10 \text{ GeV}, \quad |\eta_\ell| < 2.5. \quad (8)$$

We have also included the irreducible QCD backgrounds to $pp \rightarrow W_0 Z_0 qq'$ (cf. dashed curve in Fig. 3 below).

For computing the SM EW backgrounds, we need to specify the reference value of the SM Higgs mass M_H . Because the SM Higgs scalar only contributes to the t -channel in $pp \rightarrow qq' W_0 Z_0$, we find that varying the Higgs mass in its full range $M_H = 115 \text{ GeV} - 1 \text{ TeV}$ has little effect on the SM background curve. Hence we can simply set $M_H = 115 \text{ GeV}$ in our plots without losing generality.

The process $pp \rightarrow W_0 Z_0 qq'$ is a $2 \rightarrow 4$ scattering process including both fusion and non-fusion contributions, where the former are the diagrams with a fusion subprocess $W_0 Z_0 \rightarrow W_0 Z_0$. Using the improved cuts (6)-(8), we have computed the $W_0 Z_0$ invariant mass ($M_{W_0 Z_0}$) distribution in both unitary gauge and 't Hooft-Feynman gauge as depicted in Fig. 2(a). The final result (the sum of the fusion and non-fusion pieces) is identical in the two gauges, as shown in Fig. 2(b).

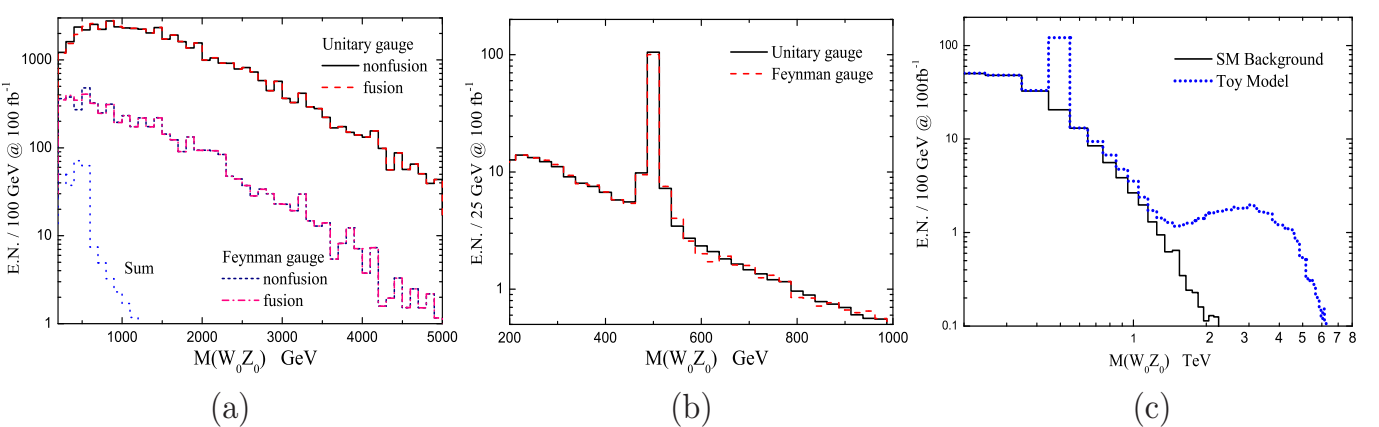


FIG. 2: Invariant-mass distribution $M_{W_0 Z_0}$ in $pp \rightarrow W_0 Z_0 qq'$ for $M_{W_1} = 500 \text{ GeV}$: (a). fusion (dashed) and non-fusion (solid) contributions in the unitary gauge, fusion (dashed-dashed) and non-fusion (dashed-dotted) contributions in the 't Hooft-Feynman gauge, and the sum of fusion and non-fusion contributions in both gauges which coincide (dotted); (b). comparison of the summed contributions (after cancellation) between the two gauges, in the MHLML; (c). same as (b), but for a toy model based on a sum-rule approach (like that in Ref. [9]) which explicitly violates gauge-invariance.

Strikingly, we have revealed an extremely precise and large cancellation between the fusion and non-fusion contributions, as required by the exact gauge-invariance

of the MHLML Lagrangian [19]. This manifest gauge-invariance of the MHLML Lagrangian is crucial for obtaining the correct collider phenomenology and nontrivially

verifies the consistency of our analysis. Note that the separate fusion and non-fusion contributions are gauge-dependent and a large precise cancellation occurs *only if they are rigorously combined*, i.e., all the new physics contributions to the gauge-couplings of W_0/Z_0 and W_1/Z_1 as well as their couplings to the light fermions *must be consistently included*. The curves shown in Fig. 2(a)(b) come from the Higgsless model and no SM Higgs boson is invoked [20]. To be concrete, we see that at $M_{W_0Z_0} = 1$ TeV, the cancellation in the unitary gauge is a factor of $2400/2.3 \simeq 1043$, while that in 't Hooft-Feynman gauge is a factor of $195/2.3 \simeq 84.7$. We stress that these cancellations cannot be inferred without a truly gauge-invariant model.

As a comparison, we also show, in Fig. 2(c), the summed result of the fusion and non-fusion contributions in unitary gauge for a naive toy model that is not gauge invariant. Following the 5d sum rule approach [9], we assume that W_0 and Z_0 have exactly the SM-couplings to light fermions while W_1 and Z_1 do not couple to the fermions. Next, one has to estimate the gauge boson self-couplings. There are at least 3 self-gauge-couplings (involving W_0 - W_0 - Z_0 - Z_0 , W_0 - W_0 - Z_0 and W_1 - W_0 - Z_0 vertices) which cannot be equal even after assuming all higher KK modes are fully decoupled. But only two sum rules from requiring E^4 and E^2 cancellations in $W_0Z_0 \rightarrow W_0Z_0$ can be derived; the E^2 sum rule may be used to estimate the W_1 - W_0 - Z_0 coupling (ignoring all higher KK modes) and then the E^4 sum rule could determine the W_0 - W_0 - Z_0 coupling if one assumes the W_0 - W_0 - Z_0 - Z_0 coupling equals the SM-value. With this setup, we recompute Fig. 2(a) and plot the summed results in Fig. 2(c); it shows that the precise cancellation we found for the MHL M in Fig. 2(b) is now destroyed in the high energy region $1.5 - 7$ TeV, causing a large fake peak around 3 TeV in Fig. 2(c).

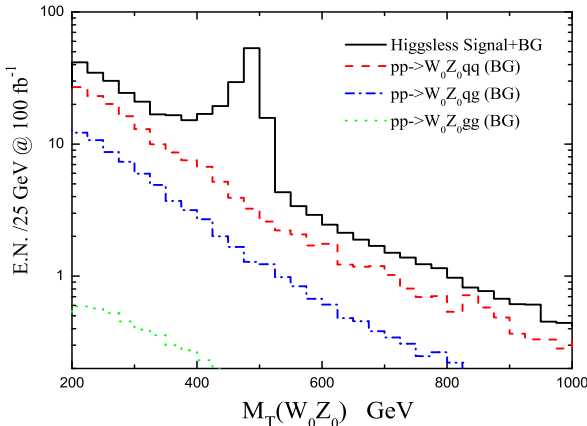


FIG. 3: Numbers of signal and background events versus the transverse mass $M_T(W_0Z_0)$ after imposing the cuts (6)-(8) for an integrated luminosity of 100 fb^{-1} .

Traditional analyses [15] of gauge-boson fusion in a strongly-interacting symmetry breaking sector have relied on using separate calculations of the signal and back-

ground. The background is calculated in the SM, while the signal could be calculated only by using a model of $2 \rightarrow 2$ Goldstone-boson scattering and applying the equivalence theorem together with effective- W approximation. The MHL M Lagrangian [8] is exactly gauge-invariant and, as we have demonstrated here, allows direct calculations of full $2 \rightarrow 4$ processes in any gauge.

In a realistic experimental analysis, one must study the transverse mass, $M_T^2(W_0Z_0) = [\sqrt{M^2(\ell\ell\ell)} + p_T^2(\ell\ell\ell) + |p_T^{\text{miss}}|^2] - |p_T(\ell\ell\ell) + p_T^{\text{miss}}|^2$ [15]. We compute both the signal and backgrounds for the $M_T(W_0Z_0)$ distribution and depict them in Fig. 3. Counting the signal and background events in the range $0.85M_{W_1} < M_T < 1.05M_{W_1}$, we further obtain the required integrated luminosities for 3σ and 5σ detections of the W_1 boson, as shown in Fig. 4.

5. Complementarity and the LHC Discovery Potential

We have performed the first gauge-invariant study of LHC signatures of the new gauge bosons predicted by the Minimal Higgsless Model (MHL M) [8]. The $W_0Z_0Z_0$ channel is of special importance due to its distinct $jj4\ell$ signals and the full reconstruction of W_1 peak (Fig. 1). We find that the simple cuts (5) can sufficiently suppress all the SM backgrounds and single out the $jj4\ell$ signals. The W_0Z_0jj channel has a larger cross section when M_{W_1} is heavy, but measuring the W_1 peak is harder due to the missing- E_T of final state neutrinos. Hence, the $W_0Z_0Z_0$ channel plays a *crucial complementary role* to the W_0Z_0jj channel for *co-discovering* W_1 bosons at the LHC. Confirming the W_1 signals in *both channels*, as well as the *absence* of a Higgs-like signal in $pp \rightarrow Z_0Z_0qq \rightarrow 4\ell qq$, will be strong evidences for Higgsless EWSB.

We summarize the 3σ and 5σ detection potential of the LHC in Fig. 4, where the required integrated luminosities are derived over the full range of allowed W_1

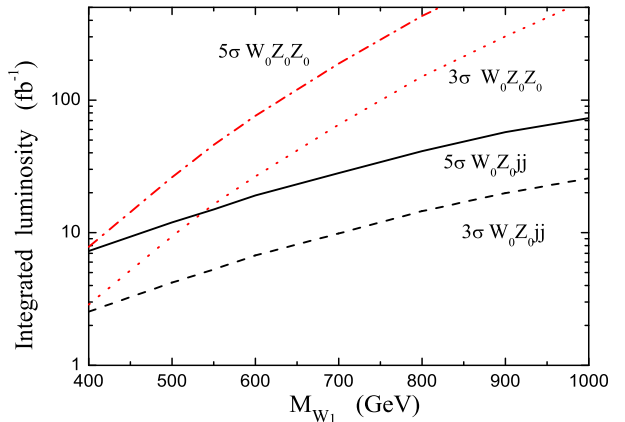


FIG. 4: Integrated luminosities required for 3σ and 5σ detection of W_1 signals as a function of M_{W_1} . The dotted and dash-dotted curves are for the $W_0Z_0Z_0$ channel, while the dashed and solid curves are for the W_0Z_0jj channel.

mass. Here we have included statistical error in determining the discovery potential; systematic error and other detector details are beyond the current scope. We find that, for $M_{W_1} = 500(400)$ GeV, the 5σ discovery of W_1 requires an integrated luminosity of $26(7.8)$ fb^{-1} for $pp \rightarrow W_0 Z_0 Z_0 \rightarrow jj 4\ell$, and $12(7)$ fb^{-1} for $pp \rightarrow W_0 Z_0 jj \rightarrow \nu 3\ell jj$. These discovery reaches will be achieved within the first few years' run at the LHC.

6. Conclusions

In this work, we have presented the first realistic and consistent study of LHC signatures for the Minimal Higgsless Model (MHLM), which is proven (through the unitary gauge and 't Hooft-Feynman gauge) to be exactly gauge-invariant. Such exact gauge-invariance was never demonstrated before in all other Higgsless studies.

In the first part of our work, we proposed and studied, for the first time, a new promising channel $WZZ(\rightarrow jj4\ell)$ for detecting new W_1 bosons in the Higgsless model. In the second part, we gave the first quantitative study of the $WZjj$ channel and its LHC-signatures of W_1 from the exactly gauge-invariant MHLM Lagrangian. In this channel we demonstrated for the first time the large cancellations between fusion and non-fusion graphs in the MHLM by *consistently including all new physics contributions* [cf. Fig. 2(a)-(b)]. We also proved that

a non-gauge-invariant Higgsless toy model does violate this large cancellation, and leads to erroneous high energy behavior of $M_{W_0 Z_0}$ [cf. Fig. 2(c)]. Therefore, it is vital to adopt exactly gauge-invariant Higgsless models such as the MHLM [8] for correctly studying LHC-phenomenology via $2 \rightarrow 4$ processes. Furthermore, our study computed not only the realistic signal events but also the correct background events (cf. Fig. 3), which are crucial for predicting the LHC discovery potential of new W_1 bosons.

We have further demonstrated the *complementarity between the WZZ and $WZjj$ channels*, which are both very promising. The LHC discovery potential of new W_1 bosons in both channels was first quantitatively predicted over the full mass-range of W_1 in Fig. 4.

Acknowledgments:

We thank Bing Zhou for discussing the LHC/ATLAS detection, and Tao Han for discussing the QCD-scale used in Ref. [18]. This research was supported by the NSF of China under grants 1062552, 10635030, 90403017, 10705017; and by the US NSF under grant PHY-0354226 as well as MSU High Performance Computing Center. The authors also acknowledge the support of the Radcliffe Institute of Advanced Study at Harvard University, the CERN Theory Institute and Fermilab Theory Department during the completion of this work.

-
- [1] C. Csaki, C. Grojean, H. Murayama, L. Pilo, J. Terning, Phys. Rev. **D69**, 055006 (2004); C. Csaki, C. Grojean, L. Pilo, J. Terning, Phys. Rev. Lett. **92**, 101802 (2004).
 - [2] R. S. Chivukula, D. A. Dicus, H.-J. He, Phys. Lett. B **525**, 175 (2002); R. S. Chivukula, H.-J. He, Phys. Lett. B **532**, 121 (2002). R. S. Chivukula, D. A. Dicus, H.-J. He, S. Nandi, Phys. Lett. B **562**, 109 (2003).
 - [3] H.-J. He, Int. J. Mod. Phys. A **20**, 3362 (2005).
 - [4] P. W. Higgs, Phys. Lett. **12**, 132 (1964).
 - [5] N. Arkani-Hamed, A. G. Cohen, H. Georgi, Phys. Rev. Lett. **86**, 4757 (2001); C. T. Hill, S. Pokorski, J. Wang, Phys. Rev. **D64**, 105005 (2001).
 - [6] R. S. Chivukula, E. H. Simmons, H.-J. He, M. Kurachi, M. Tanabashi, Phys. Rev. D **70**, 075008 (2004); Phys. Rev. D **71**, 035007 (2005).
 - [7] R. S. Chivukula, E. H. Simmons, H.-J. He, M. Kurachi, M. Tanabashi, Phys. Rev. D **71**, 115001 (2005).
 - [8] R. S. Chivukula, B. Coleppa, S. Di Chiara, E. H. Simmons, H.-J. He, M. Kurachi, M. Tanabashi, Phys. Rev. D **74**, 075011 (2006).
 - [9] A. Birkedal, K. Matchev and M. Perelstein, Phys. Rev. Lett. **94**, 191803 (2005).
 - [10] R. Casalbuoni, S. De Curtis, D. Dominici, and R. Gatto, Phys. Lett. B **155**, 95 (1985).
 - [11] R. S. Chivukula, E. H. Simmons, H.-J. He, M. Kurachi, M. Tanabashi, Phys. Rev. D **72**, 015008 (2005); D **72**, 095013 (2005).
 - [12] ATLAS Physics TDR, *Detector and Physics Performance – Technical Design Reports*, CERN/LHCC/99-15, vol. 1.
 - [13] J. Alwall et al., arXiv:0706.2334 [hep-ph], and Web link: <http://madgraph.hep.uiuc.edu>.
 - [14] A. Pukhov, arXiv:hep-ph/0412191; E. Boos et al., Nucl. Instrum. Meth. A **534**, 250 (2004) [arXiv:hep-ph/0403113]; P. Meade and M. Reece, arXiv:hep-ph/0703031.
 - [15] J. Bagger, et al., Phys. Rev. D **52**, 3878 (1995).
 - [16] H.-J. He, Y.-P. Kuang, C.-P. Yuan, B. Zhang, Phys. Lett. B **554**, 64 (2003); B. Zhang, Y.-P. Kuang, H.-J. He, C.-P. Yuan, Phys. Rev. D **67**, 114024 (2003).
 - [17] H.-J. He et al., work in preparation.
 - [18] T. Han, G. Valencia, S. Willenbrock, Phys. Rev. Lett. **69**, 3274 (1992).
 - [19] It is well-known that in any perturbative expansion up to a finite order, the width of an s -channel resonance (such as W_1 in the MHLM or Higgs boson in the SM) will violate gauge-invariance due to neglecting the higher order effect. But our study explicitly shows that, for the small Γ_{W_1} in (3) as predicted by the MHLM, such an effect is not visible up to energies well above 1 TeV in current numerical analysis.
 - [20] This contrasts with the case of the SM, where Higgs-exchange is crucial to cancel the order E^2 fusion-diagram contributions to $WZ \rightarrow WZ$.